

Adjoint sensitivity of the forecast to TOVS observations

By NADIA FOURRIÉ*, ALEX DOERENBECHER, THIERRY BERGOT and ALAIN JOLY

Centre National de Recherches Météorologiques, France

(Received 2 October 2001; revised 10 June 2002)

SUMMARY

The adjoint sensitivity to observations which is based on the adjoint operator of the variational assimilation process is used here on ten cases of the Fronts and Atlantic Storm-Track EXperiment (FASTEX), conducted in January and February 1997. It is used as a diagnostic tool allowing one to indicate which TIROS-N (Television Infrared Observation Satellite) Operational Vertical Sounder (TOVS) channels have an influence on the forecast of mid-latitude lows. In order to study the effects of the observations on the modification of the forecast from the guess, a particular cost function has been chosen: the energy of the difference between the forecast derived from the guess and the one resulting from the analysis. The first part of the paper deals with the sensitivity to the assimilated TOVS observations for the intensive observation period 17 of FASTEX. Then, the influence of TOVS data is compared with one of the other conventional datasets assimilated at the same time. After that, these results are generalized in an overview of the ten studied cases. This study highlights that the Microwave Sounding Unit and clear sky or partly cloudy High-resolution Infra-Red Sounder have the larger influence of the TOVS observations on the modification of the forecast. However, the other conventional data have a larger absolute contribution than the TOVS ones.

KEYWORDS: Adjoint operator Remote-sensed observations Variational assimilation

1. INTRODUCTION

Geostationary and polar-orbiting satellites provide global and frequent data that are assimilated in the operational weather-prediction systems. Among polar orbiting satellites, the TIROS-N† Operational Vertical Sounder (TOVS) consists of three passive vertical sounding instruments (Smith *et al.* 1979): the High-resolution Infra-Red Sounder (HIRS) with 19 channels in the infrared band and one in the visible band, the Microwave Sounding Unit (MSU) with four channels in the vicinity of 55 GHz, and the Stratospheric Sounding Unit (SSU) with three channels near 15 μm . The difficulties of the assimilation of these brightness temperatures result from the nonlinear and complex relation between the numerical weather prediction (NWP) model variables and the remote-sensed observations. Numerous studies about TOVS data impact with variational assimilation schemes have already been carried out (see, for example, Andersson *et al.* 1998; Klinker *et al.* 2000). They show that the TOVS observations have a major positive impact on the forecasts over the southern hemisphere. A lighter positive impact of those observations is also noticed over the northern hemisphere, in spite of all the numerous conventional observations that irregularly spread in time and space. Thus, one can be interested in tracking this light positive impact on the forecasts back to their initial conditions and then back to the observations they come from. This has to be done by distinguishing the respective influence on the initial conditions of the different observation types such as TOVS, radiosondes, etc. However, that is a difficult task due to the non-trivial behaviour of the observations in the variational assimilation especially if the observed parameters are different from the model variables. Moreover the nonlinearities of forecasts also add some difficulties.

In order to gain some knowledge on the inner workings of the influence of the observations involved in the assimilation processes and forecasts, one can use specific

* Corresponding author: CNRM/GMAP, Météo-France, 42 av. G. Coriolis, 31057 Toulouse Cedex, France.
e-mail: Nadia.Fourrie@cnrm.meteo.fr

† Television Infrared Observation Satellite.

© Royal Meteorological Society, 2002.

approaches such as adjoint-based techniques: the computation of the sensitivity of the forecast to the observations (Baker and Daley 2000; Doerenbecher and Bergot 2001).

These last authors have developed this tool in order to document the impact of the additional observations of the Fronts and Atlantic Storm-Track EXperiment (FASTEX, Joly *et al.* 1999) and to study the impact of targeted observations from a critical point of view (Doerenbecher and Bergot 2001). The extra observations of this experiment consist of adaptive observations (dropsondes) launched in meteorological sensitive areas, and special observations (radiosondes at 6 UTC and 18 UTC, and radiosondes from ships located over the northern Atlantic Ocean). Used as a diagnostic tool (after the observations have been made), the sensitivity to the observations allows one to evaluate the potential ability of each observation (involved in the assimilation process) to influence the forecast (or one specific forecast aspect \mathcal{J}) in a single adjoint calculation. From the theoretical definition of the adjoint-based approach, this sensitivity can provide a linear estimate of the influence on the forecast of one (or a group of) observation(s), in the presence of all the other ones. This approach is very different from most published impact studies that usually evaluate the efficiency of observations by adding or removing observations.

For a better understanding of the TOVS data assimilation, we propose to use the diagnostic tool of the sensitivity to observations. The question that this article intends to answer is: 'Which TOVS channel has an effect on the modification of the forecast of the mid-latitude lows and storms? Finally, how does this influence of TOVS data compare with the influence of other conventional data?'

In section 2, the principles and the framework of the sensitivity to observations are summarized in the context of the three-dimensional variational (3D-Var) data-assimilation scheme. Section 3 presents the sensitivity of the forecast aspect to the TOVS and the conventional observations and their influence on the modification of the forecast. Firstly, the study of the Intensive Observation Period (IOP) 17 is considered, then a second step gathers the results provided by the study of ten FASTEX cases. Finally, in section 4, results are summarized and discussed.

2. FORMALISM

Baker and Daley (2000) and Doerenbecher and Bergot (2001) have independently developed the sensitivity with respect to the observations. The first authors explored this sensitivity in an idealized context, while the others developed this tool directly in a near-operational context. The theoretical principles of the sensitivity to observations, that includes data-assimilation properties, are extensively given by Baker (2000) and Doerenbecher (2002). Here we only give an overview of this method, so that the results may be easily understood.

(a) Variational assimilation

The theoretical framework of sensitivity to observations is data assimilation and adjoint theory. We have focused this study on the variational assimilation of the TOVS brightness temperatures, which is described by Andersson *et al.* (1994). The considered TOVS observations are the NESDIS* 120 km resolution pre-processed radiances. In the context of the operational 3D-Var assimilation at Météo-France, these observations are thinned and only one observation out of four is kept. In addition only 19 channels are assimilated (HIRS channels 1 to 8, HIRS channels 10 to 15, MSU channels 2 to 4 and

* National Environmental Satellite, Data, and Information System.

SSU channels 1 and 2) but their use depends on cloudiness and surface types. For cloudy TOVS observations, only the channels HIRS 1 to 3, MSU 2 to 4, and SSU 1 and 2, which are not contaminated by cloud effects, are assimilated. The French operational weather-forecast model ARPEGE* (Courtier *et al.* 1991) is used with the 3D-Var assimilation scheme. The assimilation resolution used in this study is a triangular spectral truncation T95 without any stretching factor ($C = 1$) corresponding roughly to a physical regular grid of 140 km and includes 31 vertical levels. The forecast model uses a T149 resolution and a stretching factor of C3.5, corresponding to a physical stretched grid of 80 km over Newfoundland and 30 km over Europe. These resolutions are lower than the ones of the operational suite for computation cost reasons but they are sufficient for the description of the studied synoptic features.

Let $\mathbf{x}^a(t_0)$ be the state vector at time t_0 , resulting from the assimilation process, let t_0 be the initial time, and t_1 be the final time. Let H be the so-called observation operator, interpolating from the model variables to the observation points, $\mathbf{x}^b(t_0)$ the guess vector, and $\mathbf{y}(t_0)$ the vector of the observations.

The 3D-Var solution, obtained after the minimization of a quadratic objective function, satisfies the optimal interpolation equation (see, for example, Lorenc 1986):

$$\mathbf{x}^a(t_0) = \mathbf{x}^b(t_0) + (\mathbf{B}^{-1} + \mathbf{H}^T \mathbf{R}^{-1} \mathbf{H})^{-1} \mathbf{H}^T \mathbf{R}^{-1} (\mathbf{y}(t_0) - H(\mathbf{x}^b(t_0))) \quad (1)$$

where \mathbf{B} stands for the guess-error covariance matrix, \mathbf{H} the linearized observation operator from H in the vicinity of the guess vector $\mathbf{x}^b(t_0)$, \mathbf{R} the observation-error covariance matrix, and $(\mathbf{y}(t_0) - H(\mathbf{x}^b(t_0)))$ is the so-called innovation vector. From Eq. (1), one can deduce the so-called assimilation operator \mathbf{K} ($\mathbf{K} = (\mathbf{B}^{-1} + \mathbf{H}^T \mathbf{R}^{-1} \mathbf{H})^{-1} \mathbf{H}^T \mathbf{R}^{-1}$) representing the Kalman gain matrix.

The analysis-error covariance matrix \mathbf{A} is defined by:

$$\mathbf{A} = (\mathbf{B}^{-1} + \mathbf{H}^T \mathbf{R}^{-1} \mathbf{H})^{-1}. \quad (2)$$

One can remark that in the operational assimilation system, \mathbf{B} and \mathbf{R} are crudely specified and therefore Eq. (2) is only an estimate of the true analysis-error covariance matrix.

(b) Sensitivity to the observations

Let \mathcal{J} be a function which depicts a specific forecast aspect. \mathcal{J} can be written $\mathcal{J}(\mathcal{M}(\mathbf{x}^a))$, where \mathcal{M} stands for the weather forecast model. Let \mathbf{L} be the tangent linear model of \mathcal{M} and let \mathbf{L}^* be its adjoint. The first-order derivation of \mathcal{J} with respect to the observation vector \mathbf{y} , according to the definition of \mathcal{J} and using Eq. (1), gives the sensitivity to the observations $\nabla_{\mathbf{y}} \mathcal{J}$ as a function of the sensitivity to the initial conditions $\nabla_{\mathbf{x}^a} \mathcal{J}$:

$$\nabla_{\mathbf{y}} \mathcal{J} = \mathbf{R}^{-1} \mathbf{H} \mathbf{A} \nabla_{\mathbf{x}^a} \mathcal{J}, \quad (3)$$

\mathbf{x}^f being the forecast state from \mathbf{x}^a . As the sensitivity to initial conditions is linked with the gradient with respect to the forecast state \mathbf{x}^f by the relation $\nabla_{\mathbf{x}^a} \mathcal{J} = \mathbf{L}^* \nabla_{\mathbf{x}^f} \mathcal{J}$, the previous equation becomes:

$$\nabla_{\mathbf{y}} \mathcal{J} = \mathbf{R}^{-1} \mathbf{H} \mathbf{A} \mathbf{L}^* \nabla_{\mathbf{x}^f} \mathcal{J}. \quad (4)$$

The computation of the whole \mathbf{A} matrix is not needed for the determination of the sensitivity to observations. In fact, it is only the projection of \mathbf{A} in the direction of $\nabla_{\mathbf{x}^a} \mathcal{J}$

* Action de Recherche Petite Echelle et Grande Echelle.

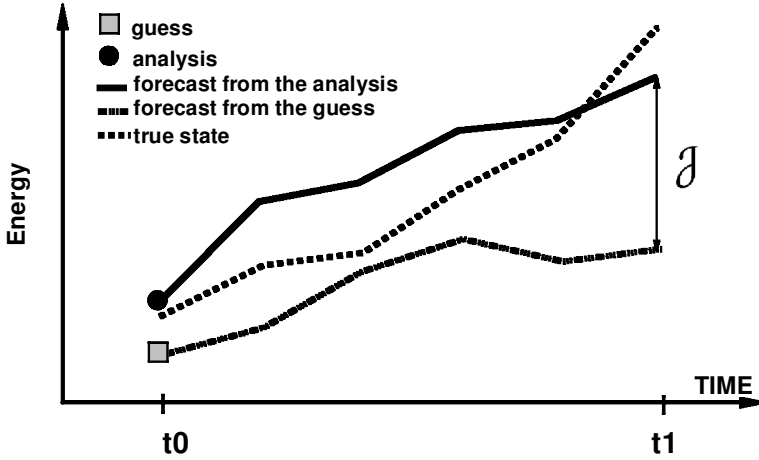


Figure 1. Principle of the cost function chosen for this study.

that has to be accurate. Following the work of Fisher and Courtier (1995), an accurate estimate of this matrix in the unstable direction of the sensitivity in an operational 3D-Var context is obtained with the update of the \mathbf{B} matrix by a low-rank matrix which is composed by a set of N update vectors. If \mathbf{V} is the rectangular matrix whose columns are the N update vectors, then \mathbf{A} is evaluated following the formula:

$$\mathbf{A} \simeq \mathbf{B} - \mathbf{V}\mathbf{V}^T. \quad (5)$$

An exhaustive study of the quality and the validation of the computation of $\mathbf{A}\nabla_{\mathbf{x}^a}\mathcal{J}$ has been carried out by Doerenbecher (2002). A good estimate is obtained with about $N \simeq 200$ and this number of update vectors is used in this study.

(c) Choice of a cost function

The choice of the cost function \mathcal{J} depends on the kind of study that one wants to carry out. This function integrates in a single real scalar value, the forecast aspect we should focus on.

During FASTEX, the cost function ‘enstrophy’ (squared vorticity) integrated over an atmospheric layer around the 850 hPa level and a geographical area of interest was used, knowing that this cost function has been shown to be suitable for studying cyclogenesis (Bergot *et al.* 1999). Other cost functions frequently found in sensitivity works are the ‘total energy’ of the forecast error (Rabier *et al.* 1996) or the ‘averaged mean-sea-level pressure’ value (Hello *et al.* 2000) over the area of interest, also called verifying area.

In this study, one wants to evaluate the capability of TOVS data to influence the forecast, independently of the forecast improvement. Therefore we have chosen the *energy of the difference between the forecast derived directly from the guess and the one derived from the analysis* (see Fig. 1). Rather, it is really the potential of the observations to influence that part of the forecast that is controlled by initial conditions in a given flow configuration that we wish to document. Our cost function tends to remove the systematic model errors that are independent from the observations, and focuses on the ability of an observation to modify the forecast derived from the guess. The difference between both initial states is indeed only based on the assimilation of the observations.

The cost function is therefore defined as:

$$\mathcal{J} = \{\mathcal{M}(\mathbf{x}^a(t_0)) - \mathcal{M}(\mathbf{x}^b(t_0))\}^T \mathbf{P}^T \underline{\mathbf{E}} \mathbf{P} \{\mathcal{M}(\mathbf{x}^a(t_0)) - \mathcal{M}(\mathbf{x}^b(t_0))\} \quad (6)$$

where \mathbf{P} is a linear localization operator projecting any global field \mathbf{x} onto the verification region of the forecast and where $\underline{\mathbf{E}}$ is the energy norm (Rabier *et al.* 1996). The results depend therefore on the choice of the norm as it has been discussed by Klinker *et al.* (1998) and Palmer *et al.* (1998) and on the choice of \mathbf{P} . As $\mathbf{P}^T \mathbf{P} = \mathbf{P}$ and $\underline{\mathbf{E}}$ is a diagonal matrix, Eq. (4) can be approximated to first order as:

$$\nabla_{\mathbf{y}} \mathcal{J} \simeq 2\mathbf{R}^{-1} \mathbf{H} \mathbf{A} \mathbf{L}^* \underline{\mathbf{E}} \mathbf{P} \mathbf{L} \delta \mathbf{x}^a(t_0) \quad (7)$$

because $\mathcal{M}(\mathbf{x}^a(t_0)) - \mathcal{M}(\mathbf{x}^b(t_0)) \simeq \mathbf{L} \delta \mathbf{x}^a(t_0)$ under the tangent linear assumption.

An increase of the amplitude of this cost function indicates that the observations tend to increase the spread or the distance between the raw forecast without any observations (starting from the guess fields), called *first forecast* hereafter, and the forecast derived from the 3D-Var analysis of observations, called *analysed forecast*. Considering two sets of observations that produce two analyses and then two forecasts, a decrease of the cost function shows that the second set of observations tends to have less influence on the forecast. The latter remains close to the trajectory followed by the *first forecast*.

3. RESULTS

We will now present the sensitivities and the contribution functions on ten FASTEX cyclogenesis cases. In our study, the guess is provided by the guess of a 4D-Var analysis of the FASTEX field phase (Desroziers *et al.* 2003) that does not take into account the additional observations of the field phase. The results are shown for a single 3D-Var assimilation cycle. The observations have been assimilated over the wide FASTEX area (as defined for the database) included between 20°N–90°N and 140°W–40°E, an area sufficient for the study of lows over the North Atlantic Ocean.

The 3D-var analysis at the initial time takes into account the TOVS and other conventional observations, but no adaptive or special FASTEX observation (from the FASTEX observing effort) has been assimilated in order to remain close to an operational setting and to compare the respective benefits of the TOVS and of the other conventional data (as in operations). The next paragraph concentrates on a single case with some details.

(a) A case-study: the FASTEX Intensive Observation Period 17

The case-study deals with the Intensive Observation Period (IOP) 17 of the FASTEX field phase. The low of interest, the so-called ‘FASTEX cyclone’, is an especially well sampled event (Cammass *et al.* 1999). It is an example of a complex life cycle ending with explosive cyclogenesis (Baehr *et al.* 1999) at 00 UTC 20 February 1997, a strong deepening rate of 40 hPa in 24 hours and a lowest central pressure of 943 hPa. The analysis is made at 18 UTC 17 February, i.e. at the early stage of the development of the cyclone. The subsequent forecast range is 42 hours. The verification zone covers the area 50°N–60°N and 0°W–20°W; it is centred over the studied low at 12 UTC 19 February.

(i) *Sensitivity to initial conditions.* Figure 2 displays the sensitivity to the initial temperature field at 700 hPa and 300 hPa. The most sensitive region of the atmosphere

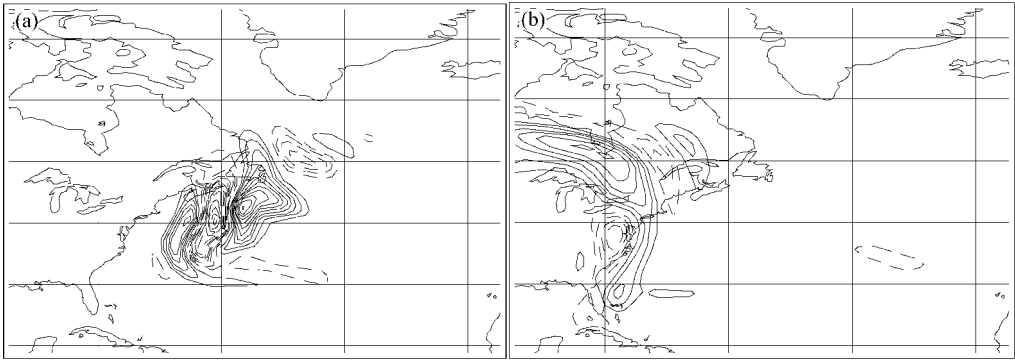


Figure 2. Sensitivity with respect to initial conditions for 18 UTC 17 February 1997 for temperature at (a) 700 hPa and (b) 300 hPa for a 42-hour forecast. Isolines every $5 \times 10^3 \text{ J m}^{-1} \text{ s}^{-2} \text{ K}^{-1}$.

is located in the low troposphere (Fig. 2(a)) over the south of Newfoundland. At 300 hPa (Fig. 2(b)) the sensitive area has a much smaller amplitude and covers a wide area south of Hudson Bay. This example illustrates the tilted structure of the sensitive zone, much like that of a singular vector and unlike that of a normal mode. One verifies here a common result of sensitivity studies: the presence of a sensitivity maximum in the low- or mid-troposphere layers.

(ii) *Sensitivity to observations.* The sensitivity of the cost function (Eq. (6)) has been computed for all the conventional data including TOVS data. Figure 3 shows this sensitivity to the HIRS 4, HIRS 15, MSU 2 and MSU 3 channel observations. Contrary to the sensitivity to initial conditions, this field is plotted at each observation position because it is computed in the observation space. The sensitivity field is here only shown for the few TOVS channels for which it is locally significant. On the same figure, the temperature component of the estimated $\mathbf{A}\nabla_{\mathbf{x}^a}\mathcal{J}$ field defined in the model space has been plotted at the level that corresponds to the weighting function maximum of the considered channel. It can be seen that the sensitivity to TOVS channels is organized in coherent regions of maximum and minimum values which correspond well to the maximum and the minimum of the temperature component of the $\mathbf{A}\nabla_{\mathbf{x}^a}\mathcal{J}$ vector, especially over the sea. This good agreement is reduced over land to the MSU 3 channel, because the low-level channels HIRS 15 and MSU 2 are not assimilated over land. The features depicted by the product of the sensitivity to initial conditions by the analysis-error covariance matrix clearly stretch over greater horizontal and vertical scales (not shown) than the classical sensitivities to initial conditions shown in Fig. 2. Figure 3 highlights that the horizontal scales implicit in the plot of the sensitivity to observations appear to be directly related to the effect of the assimilation processes on the dynamically sensitive area. The general structure of sensitive areas is simplified as shown by Fig. 3: the horizontal scale has been increased and the series of positive and negative cores is merged in a single positive core. The vertical structure is also simplified (less baroclinicity but the structure is still weakly tilted, not shown).

This is the result of the rather large-scale and simple barotropic structure functions that are included in the statistics of the 3D-Var assimilation scheme. The horizontal and vertical scales depicted in the $\mathbf{A}\nabla_{\mathbf{x}^a}\mathcal{J}$ field are then the characteristic scales of those structure functions. However, few smaller scales can be generated by the interaction of (or the combination of) the statistical influence of several nearby observations (Bergot 1999). Doerenbecher and Bergot (2001) have already studied how the assimilation

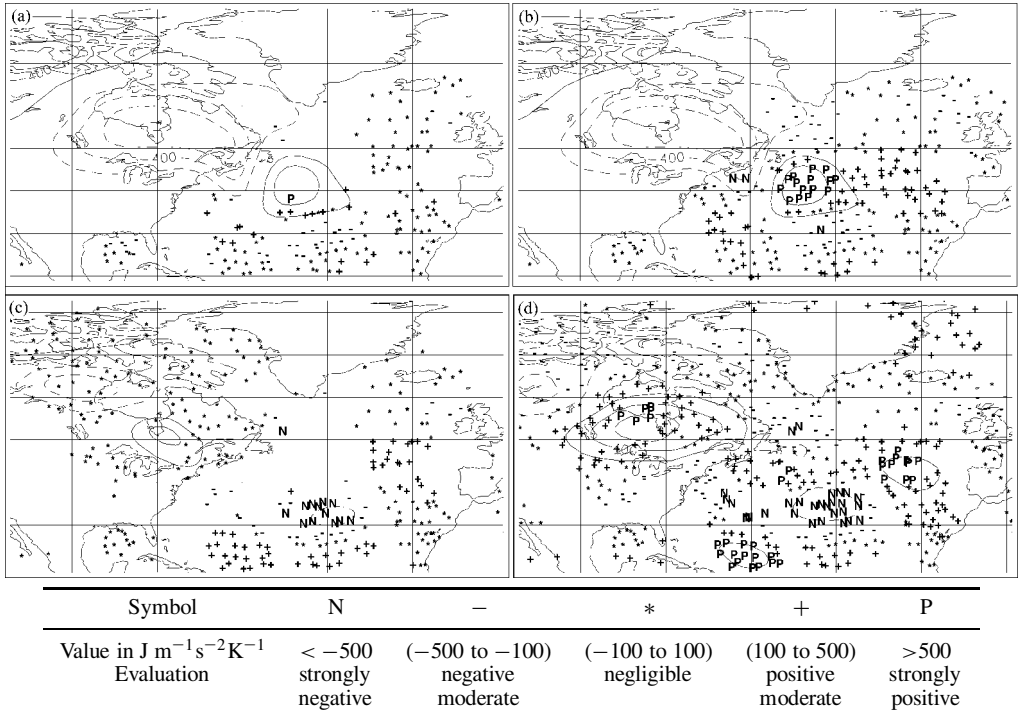


Figure 3. Sensitivity to TOVS channels for 18 UTC 17 February 1997: HIRS channel (a) 15 and (c) 4 and MSU channel (b) 2 and (d) 3, represented by the symbol corresponding to the values contained in the table above. Lines represent the temperature components of the product of the sensitivity to initial conditions by the analysis-error covariance matrix at the level corresponding to the maximum of the weighting function of the channel, (a) and (b) 700 hPa, (c) 400 hPa and (d) 300 hPa. Full lines are associated with positive values and dashed lines with negative values.

processes increase the horizontal scales and the vertical extension of the classical sensitivity field due to the structure functions of the 3D-Var assimilation, as the **A** operator basically contains a rearrangement (due to the effect of the observations) of the statistical functions of **B**.

As a consequence of the crude climatological description of the statistics of the 3D-Var, a part of the dynamical information contained in $\nabla_{x^a} \mathcal{J}$ is lost in $\mathbf{A} \nabla_{x^a} \mathcal{J}$ and then in $\nabla_y \mathcal{J}$ (the fine scales and the tilt). Moreover the large scales of $\mathbf{A} \nabla_{x^a} \mathcal{J}$ make more observations to interact with the sensitive areas. The analysis increment triggered by a given observation stretches over a sufficiently large area in order to make a part of this increment overlap any sensitive region located nearby the observation. As a consequence, the observation located nearby a sensitive area, but not included inside, can nonetheless have a non-negligible effect on the forecast. This can have a good or bad effect according to the observation and to the refinement of the assimilation scheme (not optimal in practice).

Without explicitly taking time into account within the assimilation process (case of the 4D-Var that implies different structure functions) the use of dynamically tilted structures such as $\nabla_{x^a} \mathcal{J}$ can span an unstable subspace where to describe locally a more realistic **B** within the variational data assimilation (Hello and Bouttier 2001).

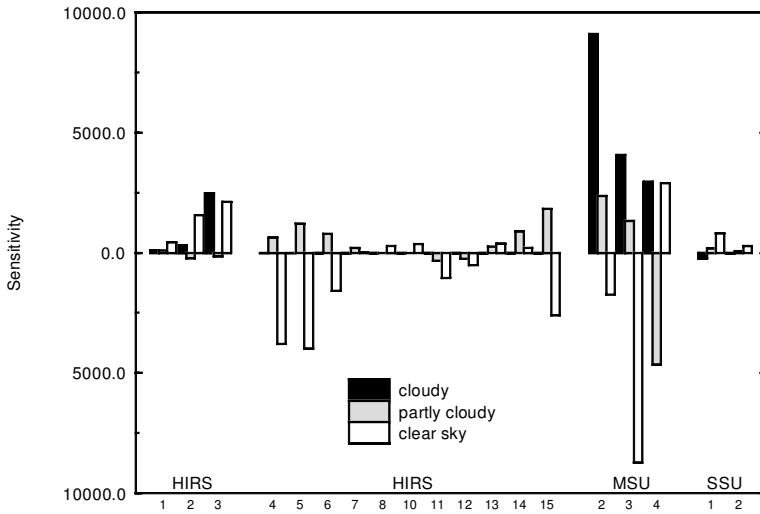


Figure 4. Sensitivity to TOVS channels (HIRS, MSU and SSU (see text)) with respect to the cloudiness of the observations for 18 UTC 17 February 1997.

The first two panels of Fig. 3 indicate that the sensitivity to the HIRS 15 observations is smaller than to the MSU 2 one. This fact is due to the lack of data over cloudy regions (the HIRS 15 channel is only assimilated in the case of clear sky or partly cloudy pixels) and to their location in the vicinity of the maximum of the gradient with respect to initial conditions modified by a part of the assimilation scheme. The influence of MSU 2 which is assimilated independently of the cloudiness over the sea is thus stronger. In addition, the sensitivity of the forecast aspect is more important for the upper-troposphere-level observations such as HIRS 4 (weighting function maximum at about 400 hPa) and MSU 3 (weighting function maximum at about 300 hPa), the data being more numerous because there is less limitation in the assimilation of the channels sounding at this level (over land and sea).

For the sake of clarity, the sensitivity to the others TOVS channels is displayed in Fig. 4. It is presented as the horizontal summation of the sensitivity to each channel with respect to its cloudiness. The modification of the forecast is mostly sensitive to the MSU data. In particular, the cloudy tropospheric observations (MSU 2) are important. The upper-troposphere clear-sky observations (MSU 3, HIRS 4 and 5) also have a large influence over the forecast modification. However, the weak sensitivity to stratospheric level TOVS channels (HIRS 1 to 3, SSU 1 and 2) results from the high sensitivity of the short-range forecast to the lower-troposphere and from the absence of cycling in the assimilation process. We therefore show that the microwave channels are crucial for the modification of the forecast derived from the guess in the case of a mid-latitude storm-track. The sensitive areas are indeed mostly located in the low- and mid-troposphere below cloudy areas (McNally 2001; Fourrié and Rabier 2002). This fact explains the ability of the MSU, which is not contaminated by the cloud effects, to modify the forecast of the IOP 17.

(iii) *'Contribution function' of the TOVS observations on the variation of the cost function.* The sensitivity to a given observation gives an indication on the ability of this observation (among all the other observations) to modify the initial conditions of the

analysed forecast and the studied cost function \mathcal{J} . It does not provide the actual role of the observation in this modification of the forecast (no observation assimilated).

Here, the computation of the cost function gives a measure (estimate) of this influence; however, it is interesting to distinguish how the observations have contributed to this value. In fact, it actually is its variation from zero as it can be interpreted as the comparison of the *first forecast* with itself, to the nonlinear evaluation of \mathcal{J} that is the comparison of the *analysed forecast* with the *first forecast*.

The definition of the adjoint sensitivity gives:

$$\delta\mathcal{J} = \langle \nabla_{\mathbf{y}}\mathcal{J}; \mathbf{y}(t_0) - H(\mathbf{x}^b(t_0)) \rangle \quad (8)$$

which is the estimate of the variation of \mathcal{J} due to the measured departure between the first guess and the observations; but it is also a first-order estimate of \mathcal{J} in that particular case of cost function. It is the summation (over all the observations y_i) of the single product $\delta\mathcal{J}_{y_i} = \nabla_{y_i}\mathcal{J} \cdot \mathbf{d}_i$, where \mathbf{d}_i stands for the innovation for the single observation y_i : $\mathbf{d}_i = y_i(t_0) - H_i(\mathbf{x}^b(t_0))$. $\delta\mathcal{J}_{y_i}$ combines the potential of a single observation (sensitivity) with the realization (in a statistical sense) of the measure of $y_i(t_0)$.

Then, for a given sensitivity, if an observation is far from the guess, its influence will be greater (greater \mathbf{d}_i) than if it is not the case. Moreover, the sign of the innovation can change the sign of the contribution $\delta\mathcal{J}_{y_i}$ when compared with the sign of $\nabla_{y_i}\mathcal{J}$.

To study the relative influence of the observation types (or TOVS channels) to the variation of the cost function \mathcal{J} , we define a new function of any partition P of the observations: that is the linear contribution to the variation of \mathcal{J} . Let \mathcal{F} be this partial summation of the $\delta\mathcal{J}_{y_i}$ over the k subsets of that partition of the observation vector:

$$\mathcal{F} = \sum_{k=1}^{M_p} \mathcal{F}_k \quad (9)$$

where M_p is the number of subsets of observations following the partition P of the observation vector \mathbf{y} . If N_{kk} is the number of observations in the subset k , let \mathcal{F}_k be:

$$\mathcal{F}_k = \sum_{i=1}^{N_{kk}} \delta\mathcal{J}_{y_i}. \quad (10)$$

\mathcal{F}_k is called the 'partial contribution function of the subset k '. Nevertheless, each subset can be divided into l sub-subsets as requested for any particular study (as for Fig. 4).

The subsets can be a choice of TOVS channels or the different assimilated observation types. Those linear estimates of the \mathcal{F}_k components should always be compared with the total $\delta\mathcal{J}$ (cf. Eq. (8)) estimate. Indeed, if the whole observation vector \mathbf{y} is considered we have $\delta\mathcal{J} = \mathcal{F}$.

Thus a negative contribution (i.e. component of \mathcal{F}) illustrates the 'antagonism' of the considered subset against the effect of the other observations in order to keep the *analysed forecast* closer to the *first forecast* that the other observations apparently suggest. Conversely, a positive contribution will imply the shift of the *analysed forecast* away from the *first forecast*. It is worth stressing that this function \mathcal{F} is computed after the observations have been made and that it indicates the actual role played by the observations in the variation of the cost function \mathcal{J} , under this assumption.

Figure 5 displays the contribution function corresponding to the sensitivity to the observations of Fig. 3. This figure shows that the regions of strong contribution

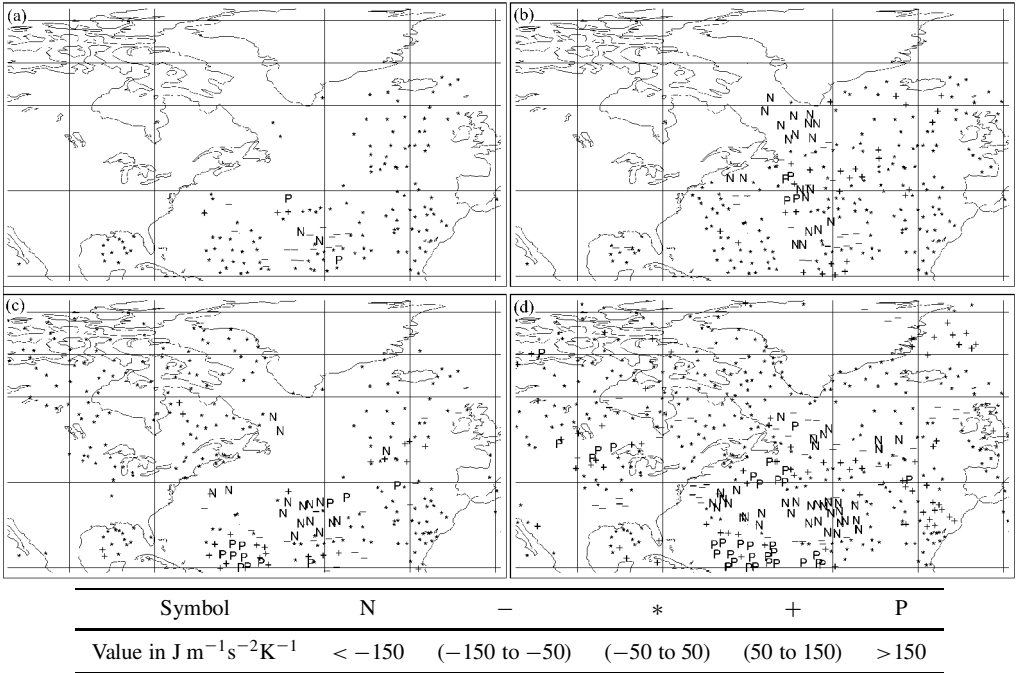


Figure 5. Contribution function of the TOVS channels for 18 UTC 17 February 1997: HIRS channel (a) 15 and (c) 4 and MSU channel (b) 2 and (d) 3. Symbols correspond to the above table.

correspond generally to areas where the sensitivity of the forecast is important. In the case of MSU 2 (Fig. 5(b)), there is a region of strong negative contribution located to the south-east of Greenland where no region of sensitivity extrema is present. In addition, an area of positive contributions of HIRS 4 channel is present between 20°N and 30°N and 50°W and 70°W (Fig. 5(c)). Nevertheless, in both cases, a moderate sensitivity is observed. Such a moderate sensitivity to the observations is a necessary condition for a strong contribution to \mathcal{F} , as shown by Doerenbecher and Bergot (2001) for the targeted observations of FASTEX IOP 17. The comparison between Fig. 3 and Fig. 5 confirms, in the presence of TOVS, a result also shown by these authors: strong sensitivity is linked to strong contribution function but strong contribution function is not necessarily associated with strong sensitivity (due to the innovation vector).

The comparison with the other channels (Fig. 6) shows that the contribution function of the MSU channels is always significant and confirms the importance of these channels for the cyclogenesis forecast. In addition, the influence of the HIRS clear-sky observations has increased in comparison with those of the MSU. The results found with the individual contribution $\delta \mathcal{J}_{y_i}$ are confirmed when computing the partial contribution function \mathcal{F} : strong contribution can be due to strong sensitivity or to large innovation vector in the case of moderate sensitivity.

In conclusion, the MSU channels have the most important individual contribution function on the forecast of the low of IOP 17.

(iv) *The partial contribution function \mathcal{F} of the other observations.* Figure 7 displays the partial contribution function of the observation types used in the analysis. The PILOT (wind data) have the most important positive partial contribution function on the

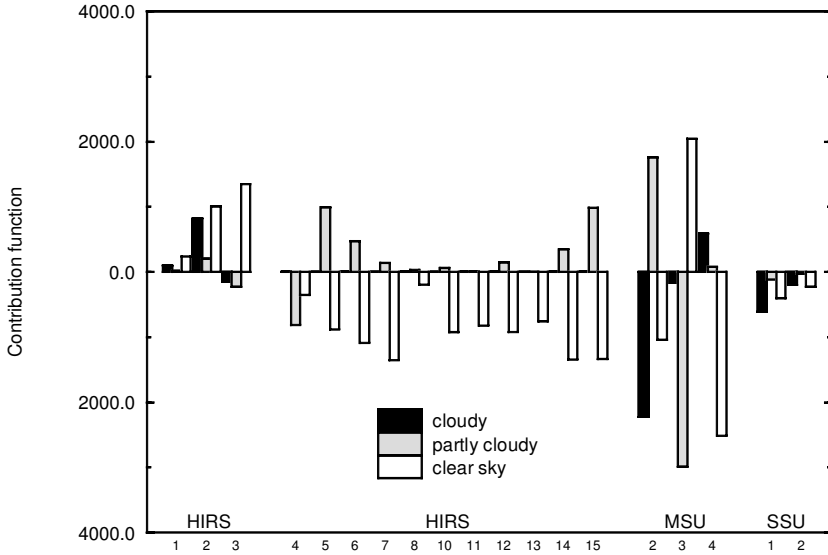


Figure 6. Contribution function of the TOVS channels (HIRS, MSU and SSU (see text)) on the variation of the cost function (in $J m^{-1} s^{-2}$).

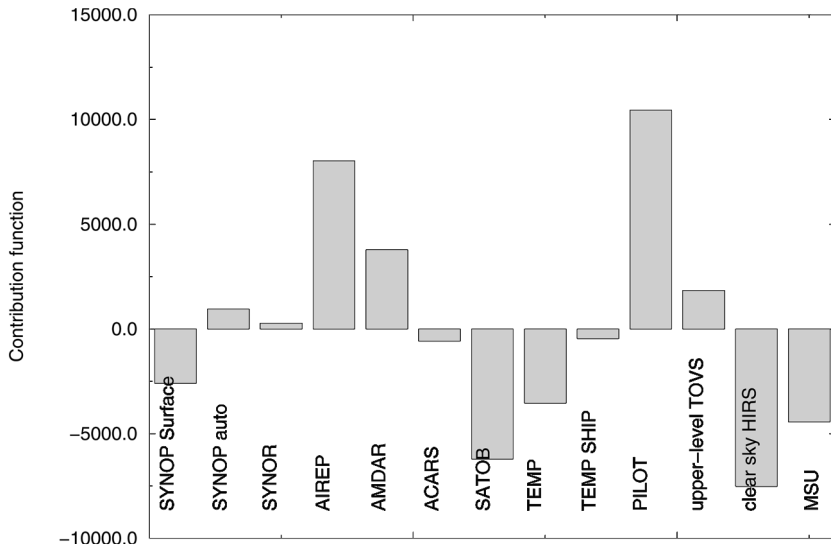


Figure 7. Contribution function of the observations on the variation of the cost function for 18 UTC 17 February 1997 (in $J m^{-1} s^{-2}$). 'SYNOP surface' represent surface data of fixed land stations; 'SYNOP auto' and 'SYNOR' are surface observations of automatic stations ('SYNOR' are specifically French data not distributed on the Global Telecommunication System); 'AIREP (AIRcraft REPort)', 'AMDAR' (Automated Meteorological DATA Report) and 'ACARS' (Aeronautical-radio-incorporated Communication Addressing and Reporting System) contain data from commercial aircraft; 'SATOB' correspond to wind observations derived from geostationary satellite measurements; 'TEMP' and 'TEMP SHIP' contain observations of radiosondes launched from fixed land stations and from ships respectively; and 'PILOT' are altitude wind data. The above message types correspond to the names of the messages following the World Meteorological Organization codes. 'Upper-level TOVS' correspond to the stratospheric channels of the TIROS-N Operational Vertical Sounder, 'clear sky HIRS' represent the clear-sky observations of the High-resolution Infra-Red Sounder, and 'MSU' correspond to the observations of the Microwave Sounding Unit.

TABLE 1. INTENSIVE OBSERVATION PERIOD (IOP), TIME, DATE, DURATION AND VERIFICATION AREA OF THE STUDIED CASES FOR TESTING TOVS BRIGHTNESS TEMPERATURE IMPACT ON THE FORECAST

IOP	Time (UTC)	Date (Feb. 1997)	Forecast	Verification area
9	18	1	30 h	55–65°N; 10–30°W
10	18	3	30 h	50–60°N; 10°W–10°E
11	18	4	30 h	50–60°N; 10–30°W
12	12	8	30 h	55–65°N; 10–30°W
15	6	15	18 h	45–60°N; 10–30°W
17a	18	17	42 h	50–60°N; 20–0°W
17b	6	18	30 h	50–60°N; 20–0°W
17c	18	18	18 h	50–60°N; 20–0°W
18a	12	22	30 h	50–60°N; 10–30°W
18b	18	22	18 h	50–60°N; 10–30°W

modification of the forecast. This is due to the wind observations of the three sites on the eastern American coast (Saint John's, Goose Bay and Halifax, not shown) that are located in the sensitive area. The clear sky or partly cloudy HIRS observations have an influence of about the same order of magnitude as the PILOT, AIREP (commercial aircraft data) or SATOB (wind derived from geostationary satellite measurements) observations. The amplitude of the partial contribution function of MSU observations can be compared with the one of the radiosondes. The MSU influence is now smaller than the HIRS one because for a given subset of TOVS observations with a comparable sensitivity, opposite innovation vectors will result in a negligible partial contribution of that subset of observations. However, the contribution function \mathcal{F} of all observations results from a compromise of the different partial contributions to the variation of the cost function. The resulting modification is unfortunately almost null for this case. In order to extend our case-study, the tool is now applied to a series of FASTEX cases.

(b) Overview

An overview of ten February 1997 FASTEX cases has been conducted. The cost function is the same as in the previous paragraph, but the verification area changes for each case in order to focus on the weather system of interest. This area is located generally over western Europe. Moreover, the energy calculation is normalized with respect to the surface unit to take into account the possible change of the size of the interest region among cases. Table 1 lists, for each case, the date of the analysis, the forecast range and the area on which the cost function is computed. The forecast range also depends on each weather system. The time of the data analysis often corresponds to a targeting flight of the FASTEX field phase, such as for the IOPs 10, 15, 17a, 17b and 18b when the TOVS observations are available over the sensitive areas. In addition, the forecast duration is mostly 30 hours. This duration is within the limits of the accepted range for the tangent linear assumption to be reasonable for adiabatic forecasts as computed in this study for the adjoint computation. Three cases correspond to short 18-hour-forecast range whereas the first assimilation of IOP 17 is followed by a 42-hour forecast.

(i) *Comparisons of the forecast errors and the cost function.* In this section, we will compare three quantities at the forecast time (Fig. 8):

- the above-defined cost function: the energy of the difference between the *first forecast* derived from the guess and the *analysed forecast* ((1) in Fig. 8);

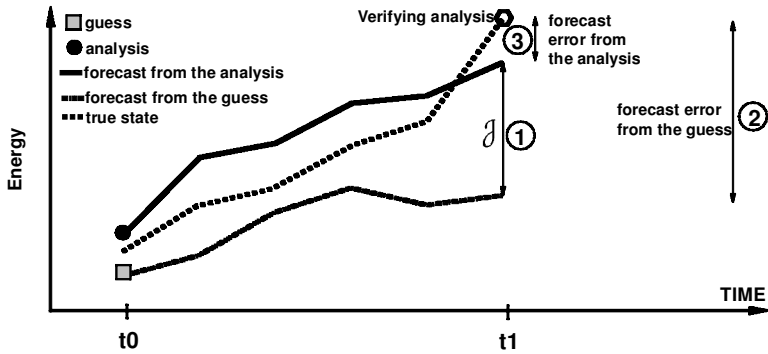


Figure 8. Principle of the three quantities compared at the final time: the cost function \mathcal{J} (1), the ‘forecast error from the guess’ (2) and the ‘forecast error from the analysis’ (3).

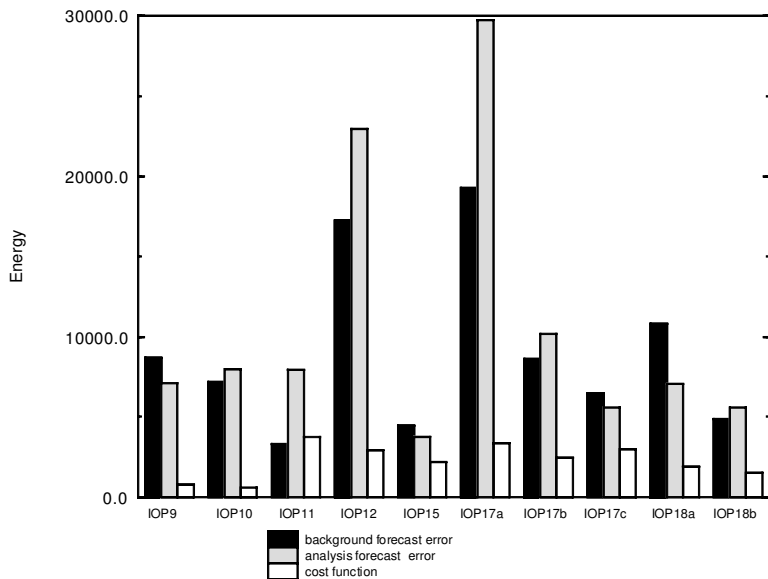


Figure 9. Forecast errors energy (in $\text{J m}^{-1} \text{s}^{-2}$) from the guess (black bars) and the analysis (grey bars), and energy of the difference between the forecast derived from the guess and the one starting from the analysis (cost function, white bars). See Table 1 for more details on the selected Intensive Observation Periods (IOPs).

- one that will be hereafter referred to as ‘the forecast error from the guess’; it is defined as the energy of the difference between the *first forecast* and the verifying 4D-Var reanalysis at the forecast time ((2) in Fig. 8); and last,
- one called ‘the forecast error from the analysis’; it is defined as the energy of the difference between the *analysed forecast* and the verifying 4D-Var reanalysis at the final time ((3) in Fig. 8).

Both forecast errors have been computed with the 4D-Var reanalysis with FASTEX data (Desroziers *et al.* 2003) in order to have the best estimation of the reality.

These three quantities are shown in Fig. 9 for the ten FASTEX cases. The contribution function does not seem to depend on the forecast error from the guess. It is worth

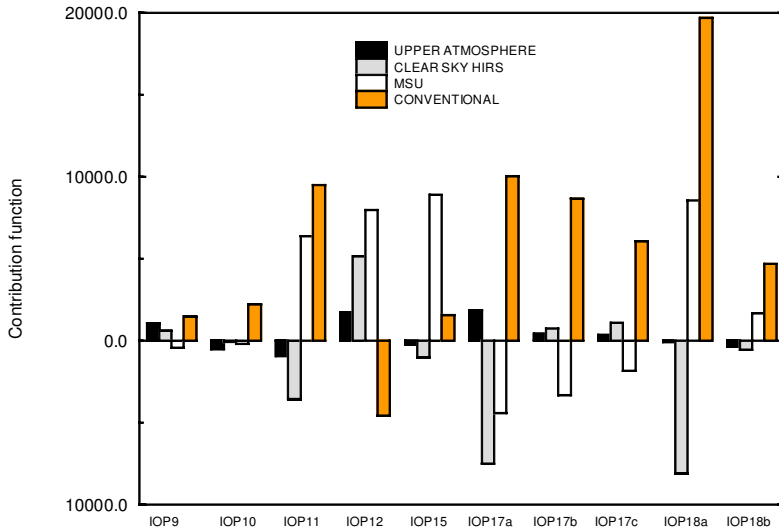


Figure 10. Contribution function (in $J m^{-1} s^{-2}$) of the observations for the studied cases. See Table 1 for more details on the selected Intensive Observation Periods (IOPs). (This figure appears in colour online.)

noticing that for six cases out of ten, the ‘forecast error from the analysis’ is larger than the ‘forecast error from the guess’. This means that the forecast errors are larger when observations are assimilated with the 3D-Var, as measured with energy. Furthermore, the dependency of the diagnostic on the forecast range has been partially documented in two cases (IOPs 17 and 18). One observes that the forecast errors naturally decrease with the reduction of the forecast range, but for IOP 18, even if for IOP 18b the ‘forecast error from analysis’ is smaller than the IOP 18a one, it is larger than the ‘forecast error from the guess’.

(ii) *Contribution function of the observations.* The contributions of the observations to the cost function are now examined. Figure 10 displays the partial contribution function of the upper-level channels, the HIRS channels used in the case of clear or partly cloudy sky, the MSU channels and the other conventional observations. One can see that the results vary from case to case. For IOPs 9 and 10, all the observations only have a weak partial contribution function on the forecast. Both cases correspond to lows that have already deepened before the period of interest. For IOPs 17 and 18, the partial contribution function of the observations seems to depend on the forecast range. Excepting IOP 12 (where their contribution function is negative) and IOP 15, conventional observations always have the larger partial contribution function, but this contribution function is of the same order as the ones of the MSU and clear sky or partly cloudy HIRS channels respectively. In addition, this contribution function is mostly positive with the exception of IOP 12. When adding all the TOVS contributions, the other conventional data have a larger contribution function than the TOVS one with the exception of IOP 12 and IOP 17a. Figure 11 displays the TOVS and the conventional contribution function as a function of the forecast error from the background. There are mainly two behaviours: a cluster of cases for which the contribution function of the conventional data is higher than the TOVS one for a small forecast error from the guess (eight cases), and two cases for which the TOVS contribution function is higher than the conventional one. It is worth noticing that these two cases (IOP 12 and IOP 17a)

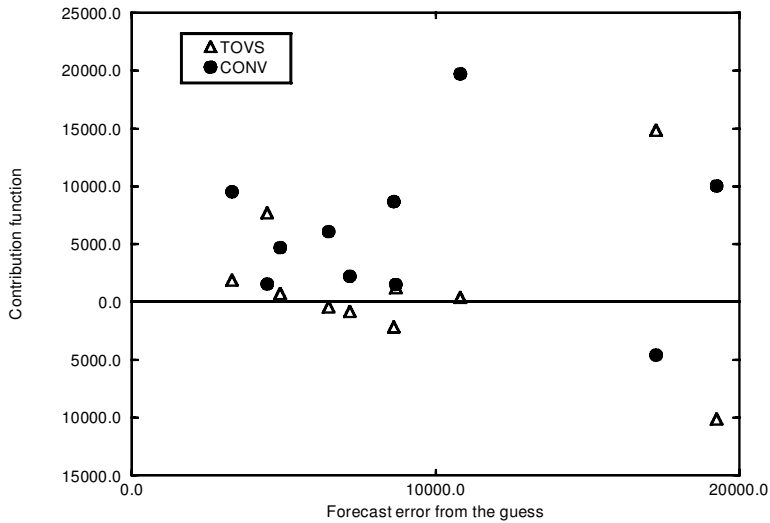


Figure 11. Contribution function (in $\text{J m}^{-1} \text{s}^{-2}$), TOVS and conventional, of the observations for the studied cases as a function of the forecast error from the guess.

correspond to the larger forecast errors from the guess. It may reveal, on one hand, that the errors develop over the ocean where there is mostly TOVS observations and, on the other hand, that TOVS observations only have a contribution function on the modification when there is a large forecast error. This result is in agreement with the work of Bergot (1999) who has already shown that an improvement of the forecast quality by the 3D-Var assimilation of the targeted data was observed when large errors were present in the background field.

It is then possible to generalize the result from the single case result (section 3(a)). The upper-atmosphere-level channels only weakly influence the forecast. The MSU and clear sky HIRS brightness temperatures contribute to influence the difference between the *analysed forecast* and the *first forecast*. MSU channels have the larger partial contribution function among the TOVS observations except for IOP 17a and IOP 18a.

(iii) *Behaviour of the observations on the modification of the forecast.* In this paragraph, the question of whether the different observation types tend to improve the forecast is addressed. Table 2 presents a summary of Figs. 9 and 10. The various types considered are clear and partly cloudy sky HIRS, MSU, together with the other conventional data which are gathered in a single type. The question is ‘does this observation type reduce the reference-forecast error resulting from running the model without observations?’. One can use the total energy to evaluate the forecast error. With such a measure, the forecast error derived from the guess is often smaller than the one from the analysis (using the short-hand expressions defined in subsection 3(b)(i)). In such a case, the *analysed forecast* can be seen as worse than the *first forecast*. As a consequence, a subset of observations with a positive component in the contribution function \mathcal{F}_k would imply a shift of the resulting forecast further from the guess, increasing the forecast error. Such a subset is noted ‘bad’. At the opposite, if the *analysed forecast* is better than the one from the guess, the same positive component to the contribution function can be seen as a corrective action of the considered subset of observations. As a consequence this subset is noted ‘good’. When one considers the cases characterized by

TABLE 2. BEHAVIOUR OF THE CLEAR SKY AND PARTLY CLOUDY HIRS OBSERVATIONS, MICROWAVE SOUNDING UNIT (MSU) CHANNELS AND OTHER CONVENTIONAL DATA FOR THE TEN INTENSIVE OBSERVATION PERIODS (IOPS)

IOP	Clear and partly cloudy HIRS observations	MSU channels	Conventional data
9	B	G	G
10	G	G	B
11	G	B	B
12	B	B	G
15	B	G	G
17a	G	G	B
17b	B	G	B
17c	G	B	G
18a	B	G	G
18b	G	B	B

(B) Indicates bad behaviour, which increases the forecast error, and (G) marks good behaviour of the observations, which decreases the forecast error.

a forecast error decreased by the addition of the observations (IOPs 9, 15, 17c and 18a), conventional data have a good behaviour. MSU observations (except for IOP 17c) have the same corrective action. In the case of an increased forecast error by the assimilation of observations, conventional data have generally a ‘bad’ behaviour and the MSU/HIRS observations have a mixed influence. In conclusion, the different observation types considered have a mixed contribution function on the improvement of the forecast.

4. CONCLUSION

The adjoint sensitivity to observations, which combines the tangent linear model \mathbf{L} , its adjoint \mathbf{L}^* , and the adjoint of the assimilation process \mathbf{K}^* , was developed in the context of the so-called targeted observations for studying the influence of extra observations during the FASTEX project (Baker 2000; Doerenbecher and Bergot 2001). The determination of the adjoint operator of the whole variational assimilation process is supported by an estimate of \mathbf{A} in the unstable direction given by the sensitivity field $\nabla_{\mathbf{x}^a} \mathcal{J}$. We have used this linear diagnostic tool in order to estimate the contribution function of TOVS observations on the forecast. This is important given the long-term tendency of increasing global coverage using remote sensing while the number of *in situ* observations decreases. The sensitivity of some forecast aspect to the observations is obtained from the sensitivity with respect to the initial conditions by the combination with the adjoint of the assimilation process. In this study, the energy of the difference between the forecast derived from the guess and the one starting from the analysis, integrated over the area covered by lows of interest, has been used as the cost function. This choice is justified by the fact that this particular function tries to get rid of systematic model errors which can be important. This choice allows one to concentrate the sensitivity calculation on the effects of the observations over the modification of the forecast from the guess fields. In addition, the actual contribution function of the observation on the modification of the forecast from the guess has been studied.

In a first step, we have shown that the dynamically sensitive areas were strongly modified by the assimilation process. Their horizontal scale and their structure have increased because of the structure functions contained in the modelled background-error statistics.

Through a case-study of IOP 17 and an overview on ten FASTEX cases, we have highlighted the critical role of the TOVS observations located near the tropopause (MSU 3 and HIRS 4) and located in the baroclinic wave guide for the mid-latitude cyclogenesis dynamics (MSU 2 and HIRS 15). However, this result depends on cloudiness of the TOVS observations, HIRS data only being assimilated for clear or partly cloudy sky. This fact weakens the contribution function of these data because of the presence of clouds over the sensitive area as shown by McNally (2001) and Fourrié and Rabier (2002).

Using the sensitivity to observations, we have shown that the 3D-Var assimilation of TOVS observations has a small contribution function on the forecast in contrast to that of other conventional data. This fact agrees with the results found by Andersson *et al.* (1998). Moreover, even if the total contribution function of all the observations over the modification of the forecast from the guess does not seem to depend on the forecast error from the guess, we have highlighted the strong contribution function of TOVS in the case of large forecast error from the guess.

Lastly, we have observed an improvement of the forecast supplied by the whole observation set for four cases out of ten.

It can be interesting to develop the sensitivity to observations in a 4D-Var context and then to extend this study to the Advanced TOVS (ATOVS) observations which were not available during the FASTEX field phase. In particular, Advanced Microwave Sounding Unit A (AMSU-A) represents a significant advance in the microwave capability: 11 sounding channels and four window channels compared to the four MSU channels and the three SSU channels. The AMSU channels numbers 3, 5, 7 and 9 correspond to the MSU channels numbers 1, 2, 3 and 4 respectively. Li *et al.* (2000) have illustrated the better retrieval accuracy obtained with the ATOVS channels in comparison with that obtained with the TOVS channels through the 1 km vertical resolution temperature retrieval. In addition, English *et al.* (2000) have shown that the impact of the assimilation of AMSU-A is smaller in the northern hemisphere than in the southern hemisphere, but it is still important because additional data are now used in the cloudy areas with AMSU.

This tool could also be used in a prognostic way for testing and choosing which channels of future sounders such as the Infrared Atmospheric Sounding Interferometer (IASI) are crucial for the forecast. The IASI will provide 8461 brightness temperature measurements for each pixel. Such numerous data are prohibited in an operational assimilation context and a channel selection appears necessary. Sensitivity to the observations could inform us about the efficiency of the IASI channels to improve the forecast and help us to find which IASI channels to use in the data-assimilation process. Even though the future infrared measurements will be more accurate, our results confirm that the use of these infrared sounders must be done in synergy with some microwave instruments. These additional data will supply useful information in cloudy regions that are crucially needed to forecast mid-latitude lows.

ACKNOWLEDGEMENTS

The authors thank the GMME/RECYF group for its friendly and technical support. FASTEX was supported by the Programme Atmosphère et Océan à Moyenne Échelle of the Institut National des Sciences de l'Univers under contracts 97/02 and 98/12, and by the European Commission under contract ENV4-CT96-0322.

REFERENCES

- Andersson, E., Pailleux, J., Thépaut, J.-N., Eyre, J., McNally, A. P., Kelly, G. and Courtier, P. 1994 Use of cloud-cleared radiances in three/four-dimensional variational data assimilation. *Q. J. R. Meteorol. Soc.*, **120**, 627–653
- Andersson, E., Haseler, J., Unden, P., Courtier, P., Kelly, G., Vasiljevic, D., Brankovic, C., Cardinali, C., Gaffard, C., Hollingsworth, A., Jakob, C., Janssen, P., Klinker, E., Lanziger, A., Miller, M., Rabier, F., Simmons, A., Strauss, B., Thépaut, J.-N. and Viterbo, P. 1998 The ECMWF implementation of three-dimensional variational assimilation (3D-Var). III: Experimental results. *Q. J. R. Meteorol. Soc.*, **124**, 1831–1860
- Baehr, C., Pouponneau, B., Ayrault, F. and Joly, A. 1999 Dynamical characterization of the FASTEX cyclogenesis cases. *Q. J. R. Meteorol. Soc.*, **125**, 3469–3494
- Baker, N. L. 2000 ‘Observation adjoint sensitivity and the adaptive-observations targeting problem’. Ph.D. Thesis, Naval Postgraduate school, Monterey, CA, USA
- Baker, N. L. and Daley, R. 2000 Observation and background adjoint sensitivity in the adaptive observation-targeting problem. *Q. J. R. Meteorol. Soc.*, **126**, 1431–1454
- Bergot, T. 1999 Adaptive observations during FASTEX: A systematic survey of upstream flights. *Q. J. R. Meteorol. Soc.*, **125**, 3271–3298
- Bergot, T. 2001 Influence of the assimilation scheme on the efficiency of adaptive observation. *Q. J. R. Meteorol. Soc.*, **127**, 635–660
- Bergot, T., Hello, G., Joly, A. and Malardel, S. 1999 Adaptive observations: a feasibility study. *Mon. Weather Rev.*, **127**, 743–765
- Cammass, J.-P., Pouponneau, B., Desroziers, G., Santurette, P., Joly, A., Arbogast, P., Mallet, I., Caniaux, G., Mascart, P. and Shapiro, M. A. 1999 FASTEX IOP 17 cyclone: Introductory synoptic study with field data. *Q. J. R. Meteorol. Soc.*, **125**, 3393–3414
- Courtier, P., Freydl, C., Geleyn, J.-F., Rabier, F. and Rochas, M. 1991 ‘The ARPEGE project at Météo-France’. ECMWF seminar proceedings, **7**, 193–231
- Desroziers, G., Hello, G. and Thépaut, J.-N. 2003 A 4D-Var re-analysis of FASTEX. *Q. J. R. Meteorol. Soc.*, **129**, in press
- Doerenbecher, A. 2002 ‘Etude de l’optimisation d’un système d’observation adaptatif pour l’amélioration de la prévision des dépressions’. Ph.D. Thesis, Université Paul Sabatier. (Available at Alex.Doerenbecher@meteo.fr)
- Doerenbecher, A. and Bergot, T. 2001 Sensitivity to observations applied to FASTEX cases. *Nonlinear Processes in Geophysics*, **8**, 467–481
- English, S. J., Renshaw, R. J., Dibben, P. C., Smith, A. J., Rayer, P. J., Poulsen, C., Saunders, F. W. and Eyre, J. R. 2000 A comparison of the impact of TOVS and ATOVS satellite sounding data on the accuracy of numerical weather forecasts. *Q. J. R. Meteorol. Soc.*, **126**, 2911–2931
- Fisher, M. and Courtier, P. 1995 ‘Estimating the covariance matrices of analysis and forecast error in variational data assimilation’. ECMWF Tech. Memo. 220. ECMWF, Reading, UK
- Fourrié, N. and Rabier, F. 2002 ‘Use of advanced sounders in cloudy conditions’. Proceedings of the Twelfth international TOVS study conference, Lorne, Australia, 27 February–5 March 2002
- Hello, G. and Bouttier, F. 2001 Using adjoint sensitivity as a local structure function in variational assimilation. *Nonlinear Processes in Geophysics* **8**, 347–355
- Hello, G., Lalaurette, F. and Thépaut, J.-N. 2000 Combined use of sensitivity information and observations to improve meteorological forecasts: A feasibility study applied to the ‘Christmas storm’ case. *Q. J. R. Meteorol. Soc.*, **126**, 621–647

- Joly, A., Browning, K. A., Bessemoulin, P., Cammas, J.-P., Caniaux, G., Chalon, J.-P., Clough, S. A., Dirks, R., Emanuel, K. A., Eymard, L., Gall, R., Hewson, T. D., Hildebrand, P. H., Jorgensen, D., Lalauette, F., Langland, R. H., Lemaître, Y., Mascart, P., Moore, J. A., Persson, P. O. G., Roux, F., Shapiro, M. A., Snyder, C., Toth, Z. and Wakamito, R. M. 1999 Overview of the field phase of the Fronts and Atlantic Storm-Track EXperiment (FASTEX) project. *Q. J. R. Meteorol. Soc.*, **125**, 3131–3163
- Klinker, E., Rabier, F. and Gelaro, R. 1998 Estimation of the key-analysis errors using the adjoint technique. *Q. J. R. Meteorol. Soc.*, **124**, 1909–1933
- Klinker, E., Rabier, F., Kelly, G. and Mahfouf, J.-F. 2000 The ECMWF operational implementation of four-dimensional variational assimilation. III: Experimental results and diagnostics with operational configuration. *Q. J. R. Meteorol. Soc.*, **126**, 1191–1215
- Li, J., Wolf, W. W., Menzel, W. P., Zhang, W., Huang, H.-L. and Achtor, T. H. 2000 Global soundings of the atmosphere from ATOVS measurements: The algorithm and validation. *J. Appl. Meteorol.*, **39**, 1248–1268
- Lorenc, A. C. 1986 Analysis method for numerical weather prediction. *Q. J. R. Meteorol. Soc.*, **112**, 1177–1194
- McNally, A. P. 2001 'The occurrence of cloud in meteorologically sensitive areas and the implication for advanced infrared sounders'. Proceedings of the Eleventh international TOVS study conference, Budapest, Hungary, 20–26 September 2000. Bureau of Meteorology Research Centre, Melbourne, Australia
- Palmer, T. N., Gelaro, G., Barkmeijer, J. and Buizza, R. 1998 Singular vectors, metrics and adaptive observations. *J. Atmos. Sci.*, **55**, 633–653
- Rabier, F., Klinker, E., Courtier, P. and Hollingsworth, A. 1996 Sensitivity of forecast errors to initial conditions. *Q. J. R. Meteorol. Soc.*, **122**, 121–150
- Smith, W. L., Woolf, H. M., Hayden, C. M., Wark, D. Q. and McMillin, L. M. 1979 The TIROS-N Operational Vertical Sounder. *Bull. Am. Meteorol. Soc.*, **60**(10), 1177–1187